GULF GENERAL ATOMIC

GA-10699

IRRADIATION-INDUCED DIMENSIONAL CHANGES OF H-327 FUEL ELEMENT GRAPHITE

by

H. R. W. Cobb

Prepared under
Contract AT(04-3)-633
for the
San Francisco Operations Office
U.S. Atomic Energy Commission

Gulf General Atomic Project 901 Date Published: September 9, 1971

GULF GENERAL ATOMIC COMPANY
P O BOX 608, SAN DIEGO, CALIFORNIA 92112

DISCLAIMER

CONTENTS

ABSTRACT v
1. INTRODUCTION 1
2. HTGR GRAPHITE 3
3. GRAPHITE IRRADIATIONS 8
3.1. Sample Selection 8
3.2. Sample Preparation 11
4. DIMENSIONAL CHANGES 12
5. DISCUSSION 24
6. CONCLUSIONS 29
ACKNOWLEDGMENTS 31
REFERENCES 32

FIGURES

1. Temperature versus fast fluence envelope (FSV) 2
2. Typical ETR-GETR fast fluence profile for irradiation capsules G13 and F25 through F29 10
3. Mean dimensional changes in FSV HTGR fuel block graphite samples (parallel to extrusion and axis of element) after irradiation in ETR or GETR for three to seven cycles 13
4. Mean dimensional changes in FSV HTGR fuel block graphite samples (perpendicular to extrusion and axis of element) after irradiation in ETR or GETR for three to seven cycles 14
5. Irradiation-induced dimensional changes versus mean irradiation temperature (range 100° to 160°C) for FSV fuel block grade H-327 graphite in parallel direction 15
6. Irradiation-induced dimensional changes versus mean irradiation temperature (range 100° to 160°C) for FSV fuel block grade H-327 graphite in perpendicular direction. 16
7. Dimensional change differences resulting from flux gradients across section of segmented cylindrical assemblies (capsule G13) . 18
8. Dimensional changes and dimensional change differences in cylindrical arrays of H-327 graphite (parallel orientation) due to 1-in. spatial fast flux gradient across the section 19

FIGURES (Continued)

9. Dimensional changes and dimensional change differences in cylindrical arrays of H-327 graphite (perpendicular direction) due to flux gradients 20

10. Structure of unirradiated H-327 graphite (FSV production grade). 21

11. Structure of irradiated H-327 graphite rod, 0.105-in. diameter: (a) parallel orientation, 0.73% contraction, fluence = 3.7 x 10^{21} n/cm^2 (E > 0.18 MeV), temperature = 800°C; (b) perpendicular direction, 0.42% contraction, fluence = 3.7 x 10^{21} n/cm^2 (E > 0.18 MeV), temperature = 800°C 22

12. Structure of irradiated H-327 graphite rod, 0.105-in. diameter: (a) parallel orientation, 1.80% contraction, fluence = 6.7 x 10^{21} n/cm^2 (E > 0.18 MeV), temperature = ∿650°C; (b) perpendicular direction, 0.95% contraction, fluence = 6.85 x 10^{21} n/cm^2 (E > 0.18 MeV), temperature = ∿650°C. 23

13. Irradiation stress relaxation effects for a number of reactor graphites expressed as a creep constant spanning FSV temperatures. 28

TABLES

1. Typical common elemental impurity levels of Grade H-327 graphite. 4

2. H-327 production graphite uniformity (density, BAF, and CTE). . 5

3. Compressive strength of Grade H-327 graphite. 6

4. Tensile property variations in H-327 graphite 7

5. H-327 graphite irradiation history, capsules G13 and F25 through F29 9

ABSTRACT

Samples of production grade H-327 fuel element graphite have been irradiated in six capsules at fast fluences and temperatures which cover the proposed service conditions of the material in the Fort St. Vrain High-Temperature Gas-Cooled Reactor. This material exhibits no observable changes in structural integrity at fast neutron fluences of 8 to 9 x 10^{21} n/cm^2 ($E > 0.18$ MeV). Furthermore, when fabricated in the current HTGR fuel block configuration, the material will not experience expansion in the radial direction within the proposed range of service conditions. Damage gradients due to variations in radial fluence and the stress relaxation effects that result are discussed in terms of a creep constant for the material which is shown to be similar to the broad band values derived for all graphites.

1. INTRODUCTION

The core of High-Temperature Gas-Cooled Reactors (HTGRs) comprises an approximate right cylinder of arrays of graphite fuel element blocks into which are sealed columns of nuclear fuel. The current fuel element design for the Fort St. Vrain (FSV) reactor is a hexagonal sectioned block 14 in. across the flats and 31 in. in length. The array of 216 fuel holes and 108 coolant holes in the blocks is arranged to give a maximum thickness of approximately 0.75 in. of graphite between adjacent line sources of neutrons, with the bulk of the fuel holes disposed to provide a graphite thickness of not more than 0.25 in. The graphite acts as a structural member of the core, a heat transfer medium, and a fast neutron moderator. Graphite undergoes property changes during fast neutron irradiation with the result that the Young's modulus and ultimate mechanical strength are increased, the coefficient of thermal expansion (CTE) is changed, and the thermal conductivity is reduced. Such fast neutron irradiation effects and also the effects due to temperature are generic characteristics of graphite in general. However, the dimensional deformation produced by irradiation is a characteristic of a specific manufacturing procedure and can be at least an order of magnitude greater than that induced by pure mechanical loading without fracture. The first core loading of fuel blocks for the FSV reactor will be manufactured from Great Lakes Carbon Corporation GLCC grade H-327 graphite. The design parameters presented in Fig. 1 in terms of a fluence and temperature envelope of expected service conditions highlight the intent to avoid problems of changes in the fuel blocks that would result in net expansion. Since at the proposed service conditions there is an initial contraction in the dimensions of a fuel block before the onset of expansion, the measured changes for a given fluence are a prerequisite for any predictions concerning helium coolant effects upon the temperature of the fuel and fuel blocks.

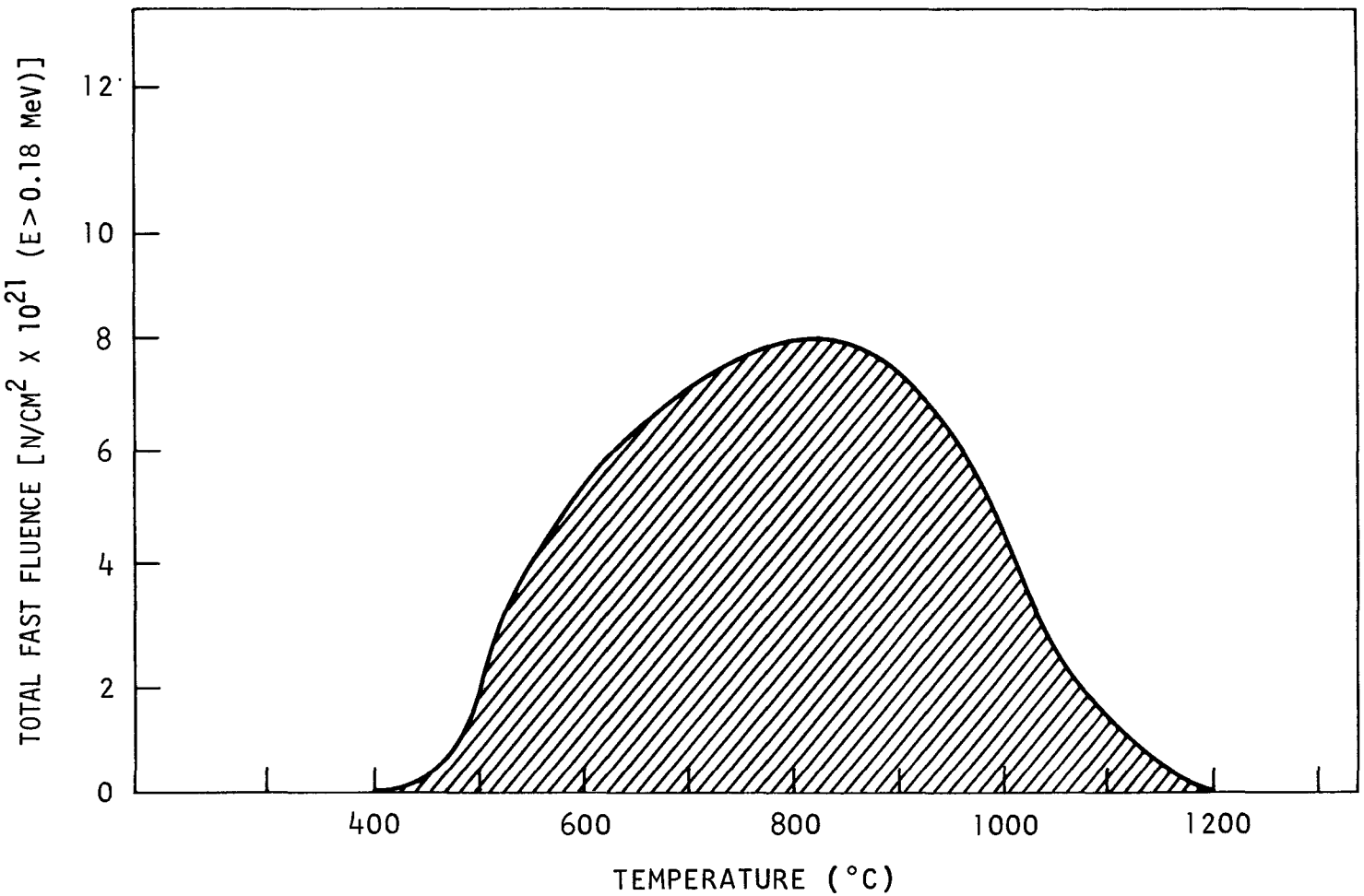

Fig. 1. Temperature versus fast fluence envelope (FSV)

2. HTGR GRAPHITE

The fuel element bodies of the FSV core are machined from 17-1/2-in. diameter by 34 in. long logs of H-327 graphite made from a blend of petrochemical needle coke particles of 60-mil maximum size bonded with a coal tar pitch. These logs are extruded, impregnated, and graphitized to produce a graphite structure with an average density of 1.78 g/cm^3 and a crystallite size of 1000 to 1200 Å. The current purification procedure during heat treatment results in a mean content of 10, 5, 2 and 1 ppm, respectively, of the most relevant common elements: iron, titanium, vanadium, and boron (Table 1).

The degree of anisotropy within a log due to the extrusion forming process is close to a value of 2 for the Bacon anisotropy factor (BAF) and CTE (Table 2). For all properties the material is considered isotropic across the section of the log, and the two principal orientations are termed "parallel" ($\parallel$) in the direction parallel to the extrusion direction and "perpendicular" ($\perp$) in the direction perpendicular to the extrusion direction. The compressive strength of H-327 graphite is relatively isotropic and uniform (Table 3) in comparison with its tensile properties (Table 4). The degree of strain induced under compression is affected by the cross-section to length ratio of the graphite, particularly in the parallel direction; and the measured value for Young's modulus is larger for the longer length samples although the proof resilience as a measure of work put into the specimens is less. The mean tensile strength for 1/2-in.-diameter rods cut from various log locations in a 1% sample of FSV fuel blocks ranges between 2325 and 877 psi, and the higher strength in the parallel direction gives a mechanical anisotropy of 1.4 to 1.9 for the strength and 2.2 to 2.6 for the chord modulus (i.e., slope of chord for stress-strain values between stresses of 250 and 500 psi). The strain at fracture in H-327 graphite is greater in the perpendicular direction, giving an isotropic ratio relative to the above relationships of parallel to perpendicular direction of 0.57 to 0.85.

TABLE 1
TYPICAL COMMON ELEMENTAL IMPURITY LEVELS OF GRADE H-327 GRAPHITE[a]

Log No.	Position	Element Concentration (ppm)									
		Al	B	Cu	Fe	Mg	Si	Ti	V	Mn	Ash[b]
10-2/694	End edge	1.0	ND	ND	ND	2.0	<10.0	4.0	ND	ND	21
3-1/705	End edge	1.0	1.0	ND	ND	2.0	<10.0	8.0	ND	ND	38
2-2/739	End edge	1.0	2.0	ND	ND	2.0	10.0	10.0	ND	ND	55
7-2/744	End edge	4.0	2.0	ND	2.0	6.0	20.0	8.0	ND	ND	77
12-2/769	End edge	1.0	1.0	1.0	1.0	4.0	20.0	10.0	ND	ND	55
12-2/956	End edge	4.0	1.0	1.0	2.0	4.0	20.0	10.0	ND	ND	472
12-1/958	End edge	ND	1.0	ND	2.0	1.0	20.0	20.0	ND	ND	317
8-2/1058	End edge	1.0	1.0	ND	ND	4.0	20.0	10.0	ND	ND	72
4-2/1959	End edge	6.0	ND	1.0	10.0	10.0	80.0	10.0	ND	ND	77
4-2/2479	End edge	4.0	1.0	1.0	1.0	6.0	20.0	10.0	ND	ND	65
3-1/2482	End edge	2.0	1.0	2.0	2.0	2.0	<10.0	6.0	ND	ND	47
42/1960	End edge	20.0	10.0	<1.0	2.0	2.0	<10.0	6.0	ND	ND	62
10/9977C	End center	2.0	ND	ND	1.0	2.0	<10.0	6.0	ND	ND	
12-1	Midlength edge	4.0	4.0	ND	1.0	4.0	20.0	8.0	ND	ND	
	Midlength ctr	1.0	ND	ND	1.0	4.0	10.0	ND	ND	ND	
0001/1743	QC edge slab	4.0	ND	ND	ND	ND	10.0	ND	ND	ND	<43
0001/2820	QC edge slab	4.0	ND	ND	ND	ND	20.0	ND	ND	ND	54
0018/1787	QC edge slab	2.0	ND	ND	6.0	ND	40.0	4.0	ND	ND	<37
0018/2511	QC edge slab	ND	ND	ND	ND	ND	ND	1.0	ND	ND	61
0175/615	QC edge slab	ND	ND	ND	ND	ND	10.0	ND	ND	ND	<32
0175/2520	QC edge slab	4.0	4.0	ND	8.0	ND	20.0	ND	ND	ND	<35
9974	QC edge slab	1.0	4.0	ND	2.0	ND	10.0	ND	ND	10.0	14
9987	QC edge slab	ND	ND	ND	1.0	ND	10.0	ND	ND	<10.0	21
9990	QC edge slab	ND	ND	ND	1.0	ND	10.0	ND	ND	<10.0	93
0060	QC edge slab	ND	ND	ND	1.0	ND	10.0	ND	ND	<10.0	93
Sensitivity, minimum content detectable		1.0	0.5	1.0	1.0	1.0	10.0	1.0	0.5	10.0	

[a] Spectrochemical analyses (except for ash analysis) were performed by GGA. Accuracy: -25% to +35% ≈ 1 σ; for 90% confidence x 1.5.

[b] Ash analysis was performed by GLCC.

TABLE 2
H-327 PRODUCTION GRAPHITE UNIFORMITY (DENSITY, BAF, AND CTE)

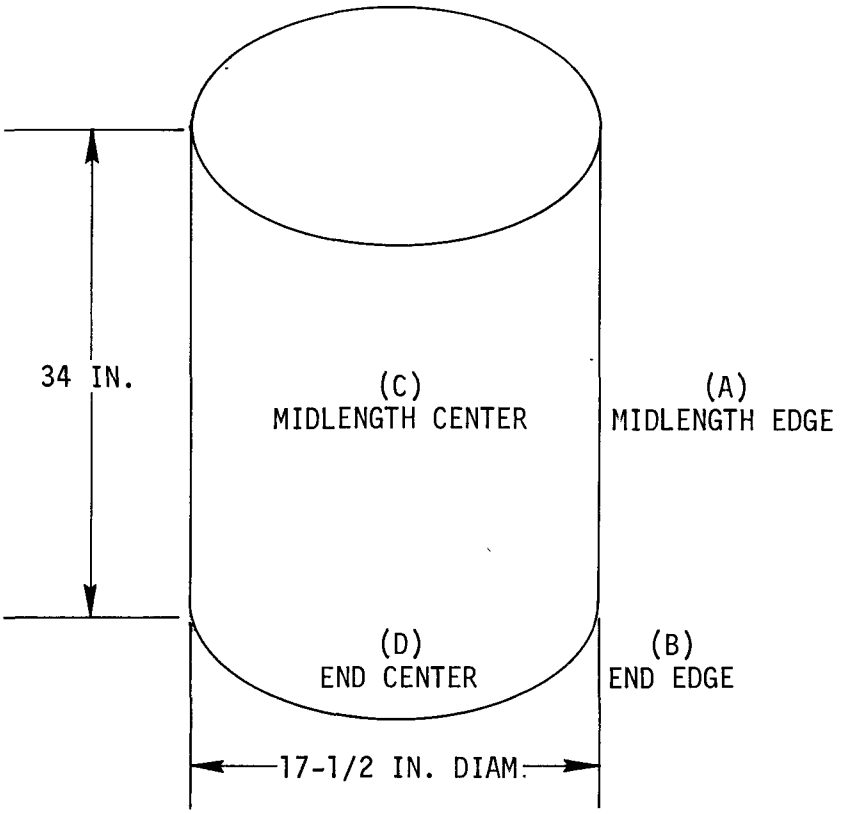

	A	B	C	D
Density, g/cm^3	1.78	1.80	1.74	1.77
BAF	(⊥) 1.03	(⊥) 1.13	(⊥) 1.30	(⊥) 1.045
CTE, mean	(∥) 3.10	(∥) 1.84	(∥) 2.75	(∥) 1.91
	(⊥) 3.29	(⊥) 3.45	(⊥) 3.32	(⊥) 3.11
CTE value between 22° and 1000°C, 10^{-6}	(∥) 1.60	(∥) 1.56	(∥) 1.58	(∥) 1.59

(⊥) Perpendicular to the extrusion direction.

(∥) Parallel to the extrusion direction.

TABLE 3
COMPRESSIVE STRENGTH OF GRADE H-327 GRAPHITE
(LOG NO. 83/9976, 13-1, 42/2163, FURNACE NO. 83, AND
LOG NO. 83/9976, 6-1, 2580, FURNACE NO. 83)

Property	Orientation						Remarks
	Parallel			Perpendicular			
	Max.	Min.	Avg.	Max.	Min.	Avg.	
Compressive stress at fracture, psi	4684	3870	4413	4989	4531	4776	(a)
	4633	4124	4446	5015	4445	4683	(b)
Strain at fracture, x 10^{-3} in./in.	40	30	33	54	44	52	(a)
	20	20	20	37	37	37	(b)
E_{max} compressive, x 10^{-6} psi	0.229	0.170	0.203	0.145	0.14	0.142	(a)
	0.575	0.288	0.401	0.233	0.232	0.236	(b)
Proof resilience, in.-lb/in.^{3}	31	20	24.5	29	28	28.5	(a)
	7.5	6.3	7.0	9.5	6	7.5	(b)

(a) Specimen size = 0.5-in. diam, 0.5 in. long.

(b) Specimen size = 0.5-in. diam, 1.0 in. long.

TABLE 4
TENSILE PROPERTY VARIATIONS IN H-327 GRAPHITE

Property	Location in Log	Mean	Std Dev	Max.	Min.	Range	Anisotropy, ∥/⊥
UTS, psi	End edge, ∥	2325	285	2920	1820	1100	1.66
	End edge, ⊥	1397	141	1678	1210	468	
	Midlength edge, ∥	2278	328	2720	1790	930	1.94
	Midlength edge, ⊥	1174	173	1370	832	538	
	End center, ∥	1793	554	2540	883	1657	1.36
	End center, ⊥	1322	338	1760	368	1392	
	Midlength center, ∥	1395	333	1920	867	1053	1.6
	Midlength center, ⊥	877	173	1100	562	538	
Strain at fracture, x 10^{-3} in./in.	End edge, ∥	2.045	0.460	2.7	1.2	1.5	0.65
	End edge, ⊥	3.128	0.622	3.8	1.3	2.5	
	Midlength edge, ∥	2.241	0.468	2.98	1.6	1.38	0.845
	Midlength edge, ⊥	2.652	0.342	3.3	2.13	1.17	
	End center, ∥	1.756	0.358	2.34	1.0	1.34	0.577
	End center, ⊥	3.042	1.028	4.5	0.75	3.75	
	Midlength center, ∥	1.395	0.211	1.73	1.1	0.63	0.687
	Midlength center, ⊥	2.028	0.502	2.85	1.3	1.55	
E chord (250-500 psi), x 10^6 psi	End edge, ∥	1.612	0.592	3.5	0.925	2.57	2.6
	End edge, ⊥	0.610	0.203	1.25	0.4	0.85	
	Midlength edge, ∥	1.417	0.51	2.7	0.926	1.77	2.48
	Midlength edge, ⊥	0.57	0.219	1.25	0.3	0.95	
	End center, ∥	1.314	0.371	2.08	0.69	1.39	2.17
	End center, ⊥	0.603	0.239	1.38	0.38	1.0	
	Midlength center, ∥	1.344	0.463	2.08	0.72	1.36	2.54
	Midlength center, ⊥	0.529	0.151	960	330	630	

3. GRAPHITE IRRADIATIONS

3.1. SAMPLE SELECTION

Samples of the current product of HTGR fuel block grade H-327 graphite have been selected at various intervals throughout the full period of graphite production for the FSV fuel blocks and irradiated in the General Electric Test Reactor (GETR) at Vallecitos, California, or in the Engineering Test Reactor (ETR) at Idaho Falls, Idaho (Table 5). Both reactors are pressurized water systems with similar mean flux levels. One capsule (G13) comprised all graphite samples, and five additional capsules (F25 through F29) contained rod-type specimens as "piggyback" samples consisting of annular cylinders of graphite containing HTGR-type fuel rods and beds of coated fuel particles. Each capsule contained four to six 1-in.-diameter, metal-clad graphite cylindrical assemblies from 2 to 6 in. long.

Dimensional change analyses of the cylinders which spanned the full cross section of the assembly were restricted to samples located in a uniform axial fast fluence profile; for most of the capsule assemblies, this profile included cells 3 and 4 (Fig. 2). Fast fluences were monitored by dosimeter wires aligned axially on the outside diameter of the assembly, and temperatures were measured by two to six thermocouples in each cell. Each cell had a thermocouple attached to the outside wall of the primary cladding, which gave continuity of temperature control through calibration with the inner thermocouple reading and mixed gas coolant flow in the event that the inner thermocouples subsequently failed. Temperature control of the gamma heating was maintained by adjustments in the composition of mixed inert gases surrounding the cylindrical assemblies in predetermined annular gas gaps. The maximum and average temperatures in the cells were recorded daily. The average temperature decreased $\sim$50°C in a fluence of 8×10^{21} n/cm^2 for the maximum time in a reactor capsule. The capsules were aligned axially parallel with a line source of fuel element neutrons less than 1 in. distant.

TABLE 5
H-327 GRAPHITE IRRADIATION HISTORY, CAPSULES G13 AND F25 THROUGH F29

Capsule	Graphite Test Assembly Cell Nos.	Number of Specimens	Specimen Shape			Temp Range (°C)	Reactor		No. of Cycles	Fluence Range [x10^{21} n/cm^2 (E>0.18 MeV)]	Time Above 165 MeV (days)
			Rods	Wedges	Cylinders		Facility	Position			
G13	1,2,3,4	132	x	x		650-1100	ETR	F13 SW	3	2.8-5.5	137
F25	1,3,4,5,6	69	x	x	x	570-1100	ETR	E5	3	1.5-4.8-6.7[(a)]	149
F26	1,2,3,4,5,6	59	x	x	x	550-1100	ETR	E5	6	3.0-7.4[(a)]	176
F27	1,2,3,4,5,6	21	x		x	700-1150	GETR	E5	4	2.8-5.65	115
F28	1,4,6	47	x		x	670-800	GETR	E5	3	1.8-4.0	87
F29	1,4,6	49	x		x	500-800	GETR	E5	7	3.3-8.7	213

[(a)] G13 samples reirradiated.

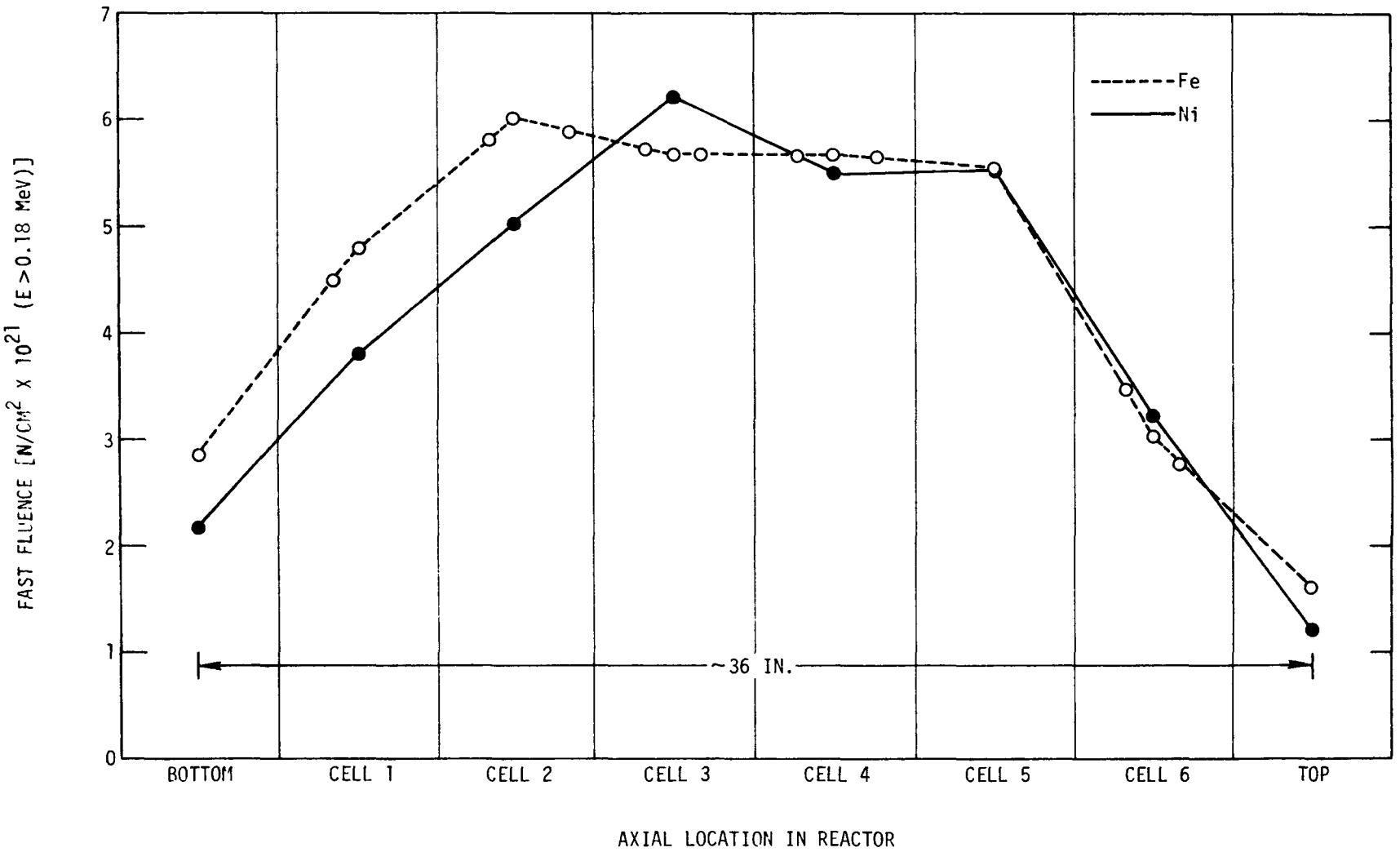

Fig. 2. Typical ETR-GETR fast fluence profile for irradiation capsules G13 and F25 through F29. Given values are for graphites in capsule F27.

3.2. SAMPLE PREPARATION

The H-327 graphite irradiation samples were in the form of ∿0.9-in.-diameter cylinders, 0.105-in. rods pitched within graphite cylinders on a Bolt Circle Diameter (BCD) of ∿0.8 in., and wedge-shaped cylindrical assemblies of segments ∿0.9 in. in diameter. The length to area ratios of the samples were approximately 2.5, 20, and 200 to 1 for the cylinders, segments, and rods, respectively. All the samples were vacuum annealed at 2000°C for 1 to 2 hr prior to assembly in the capsules. This heat treatment produced less than 0.1% change in the length of the sample after machining from the graphite logs. All samples were measured before and after irradiation to accuracies of 5 decimal places in inches.

4. DIMENSIONAL CHANGES

The physical changes due to fast neutron irradiation of production grade H-327 graphite have been measured on samples selected from logs extruded at stages covering the total materials fabrication period for FSV first core fuel elements. Dimensional changes in the material resulting from fast neutron irradiation and temperatures spanning the expected FSV service conditions are shown plotted as mean linear dimensional changes for a given measured fluence in Figs. 3 and 4. Where there is a change in the mean irradiation temperature, the subsequent dimensional change rate is complementary to the new irradiation temperature.

The most significant dimensional change parameter is the perpendicular direction, since it is the radial direction of the present HTGR core and the earliest measured fast neutron dose at which a net expansion occurs in the material (crossover) is 7×10^{21} n/cm^2 (E > 0.18 MeV) at approximately the current peak FSV mean temperature of 1075°C (950° to 1150°C range). A few samples had undergone expansions of up to 0.8% at 7.9 to 8.5×10^{21} n/cm^2 (E > 0.18 MeV), and from the onset of crossover the expansion rate is steep.

In the parallel direction (axial direction of FSV core), the maximum contraction in length occurs at those fluence levels which produce the conditions of net expansion across a fuel block, the strain difference at this fluence being approximately 5% linear contraction. The design parameters of dimensional change versus temperature are plotted in Figs. 5 and 6 to show extrapolated values to the lower FSV service temperature of 500°C and in excess of the expected peak fluence of 8×10^{21} n/cm^2 (E > 0.18 MeV).

Tests to assess the effects on irradiated dimensional change of H-327 samples cut from different positions in a log and irradiated in a cylindrical array in a uniform axial fluence showed total randomness in length changes with respect to any variations in thermophysical and mechanical strength

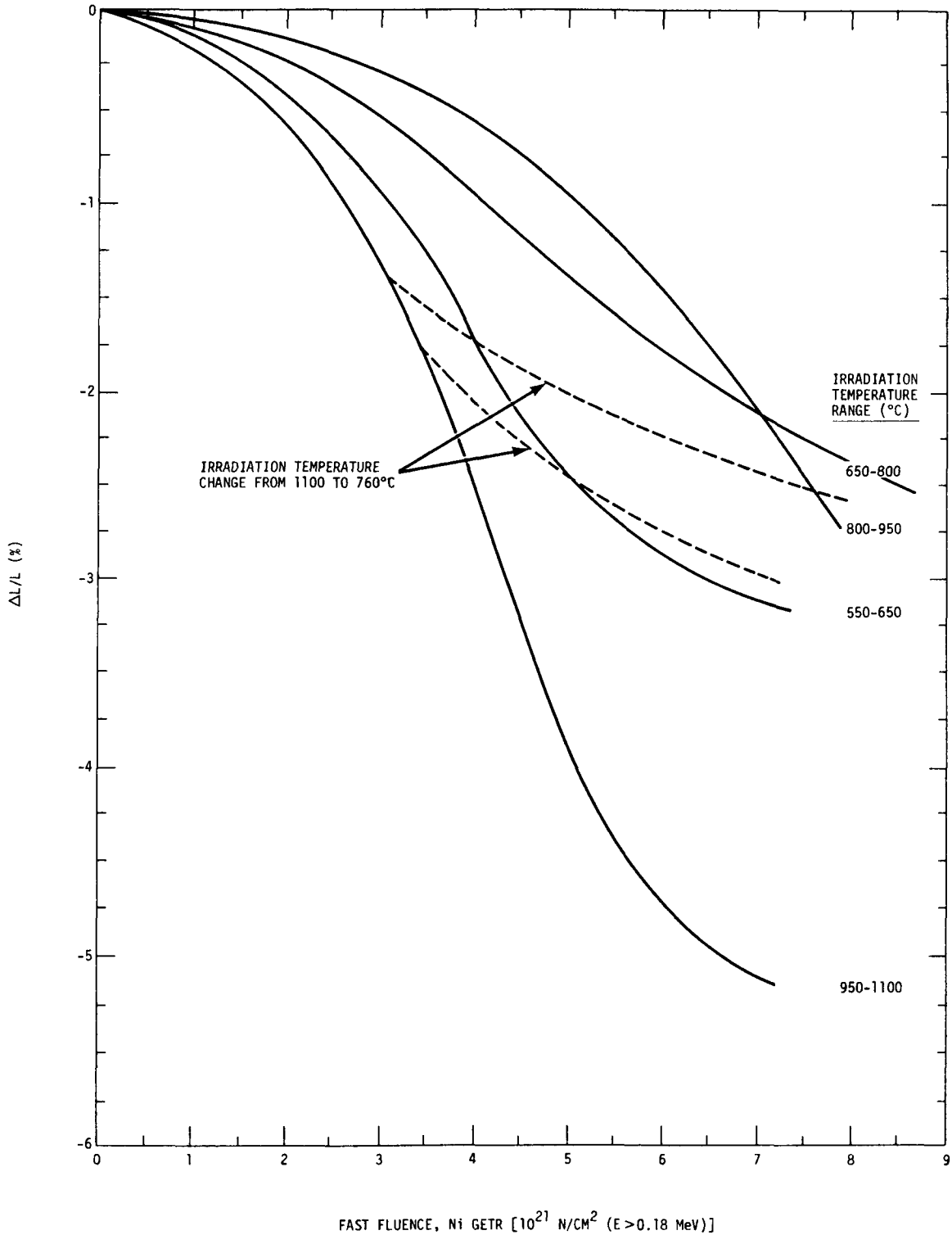

Fig. 3. Mean dimensional changes in FSV HTGR fuel block graphite samples (parallel to extrusion and axis of element) after irradiation in ETR or GETR for three to seven cycles

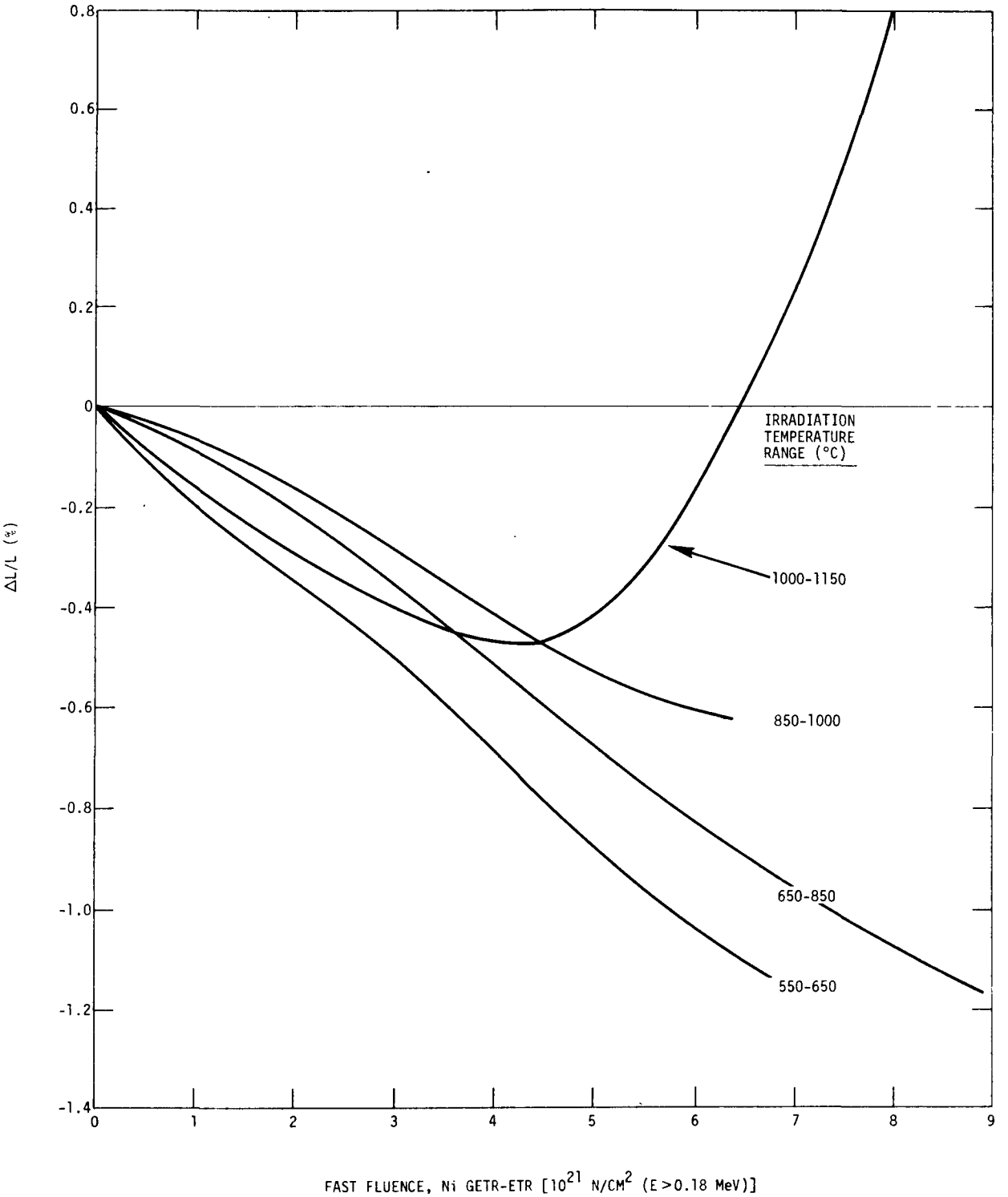

Fig. 4. Mean dimensional changes in FSV HTGR fuel block graphite samples (perpendicular to extrusion and axis of element) after irradiation in ETR or GETR for three to seven cycles

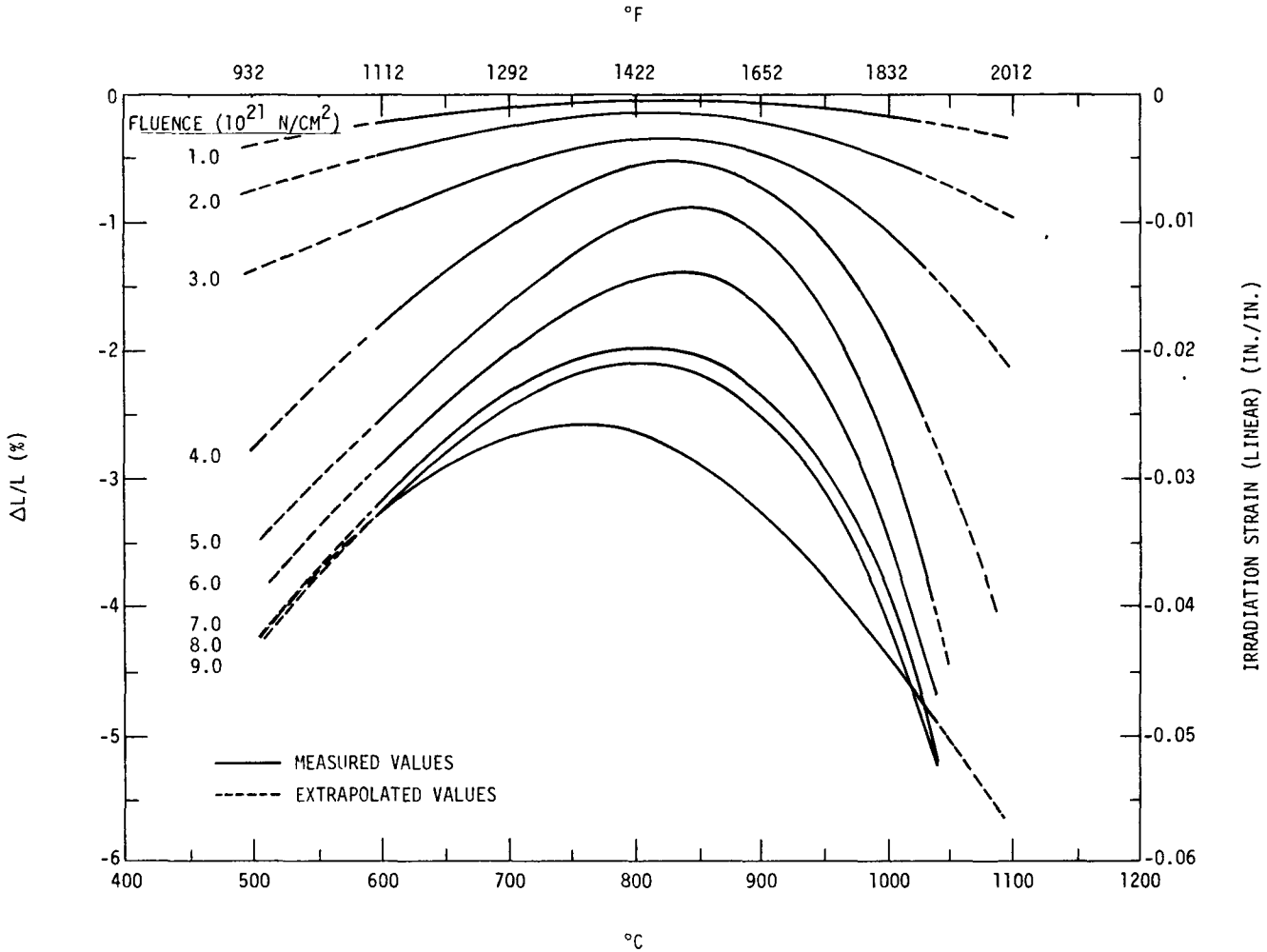

Fig. 5. Irradiation-induced dimensional changes versus mean irradiation temperature (range 100° to 160°C) for FSV fuel block grade H-327 graphite in parallel direction (axial direction in fuel block)

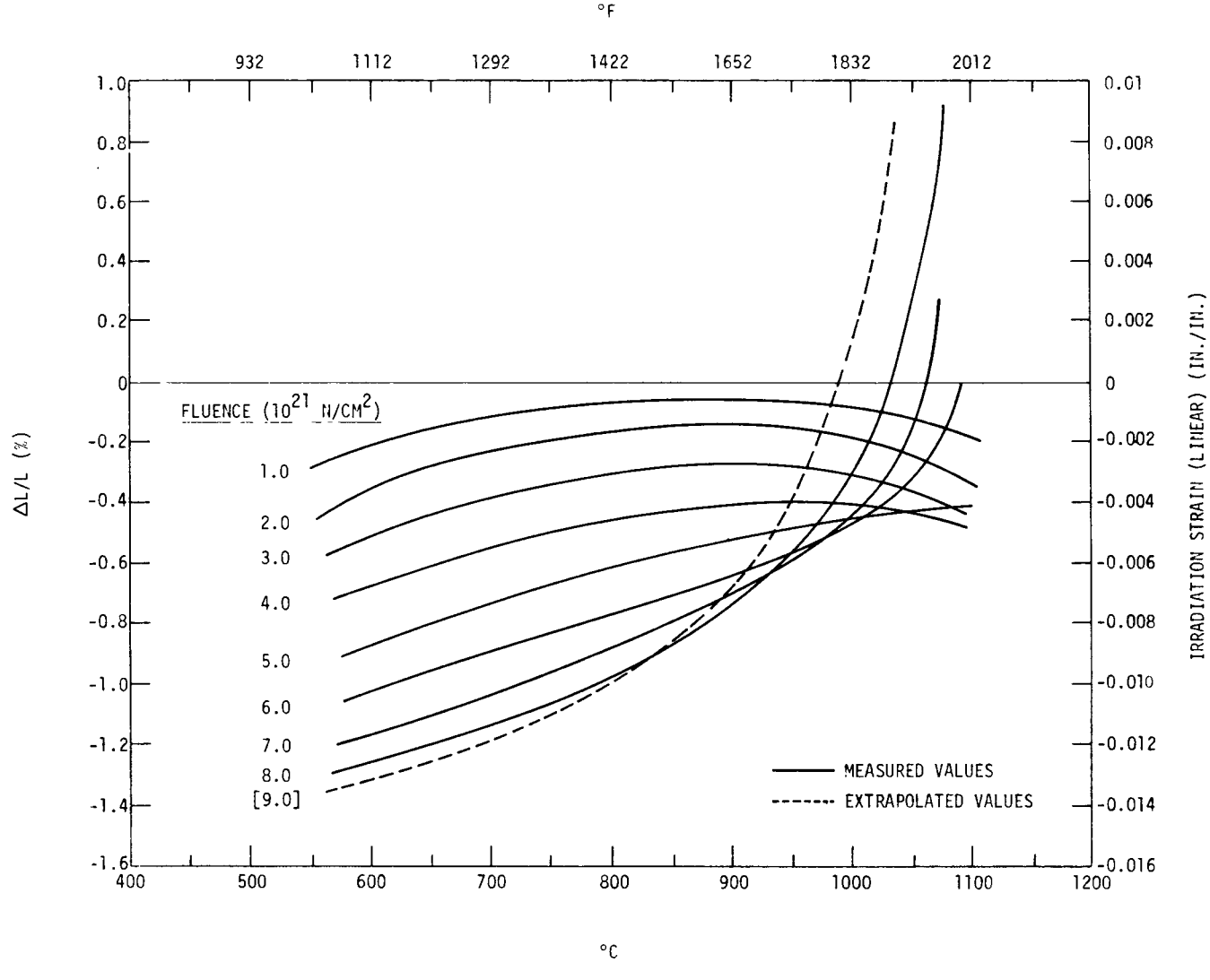

Fig. 6. Irradiation-induced dimensional changes versus mean irradiation temperature (range 100° to 160°C) for FSV fuel block grade H-327 graphite in perpendicular direction (across fuel block)

properties. Any such effects were overshadowed by what is considered to be a diametral damage gradient in the capsule. This effect was graphically shown in the all-graphite irradiation capsule G13, in which the test sections were approximately 1-in. right cylinders of graphite made up from assemblies of six 60° wedge-shaped samples (Fig. 7). The dimensional change differences have a sinusoidal distribution around the assembly, with the largest differences occurring at the highest irradiation temperature of 1100°C at a fluence of $\sim 5 \times 10^{21}$ n/cm^2 (E > 0.18 MeV). These changes reflect the developed length differences due to a diametral gradient in damage effect. The data therefore are best interpolated by plots covering a range of measured dimensional changes for a given monitored dose value from a line source of fast neutrons (Figs. 8 and 9). However, when solid cylindrical samples span similar damage gradients, the resultant measured dimensional changes are less.

A comparison of the structure of H-327 graphite prior to irradiation (Fig. 10) and after irradiation at fluences of 3.7×10^{21} n/cm^2 (Fig. 11) and 6.8×10^{21} n/cm^2 (Fig. 12) shows no discernible difference in the morphology. The irradiated samples had no measurable bow along their length, and local areas of low porosity as shown by metallography resulted in no apparent loss in integrity of the material.

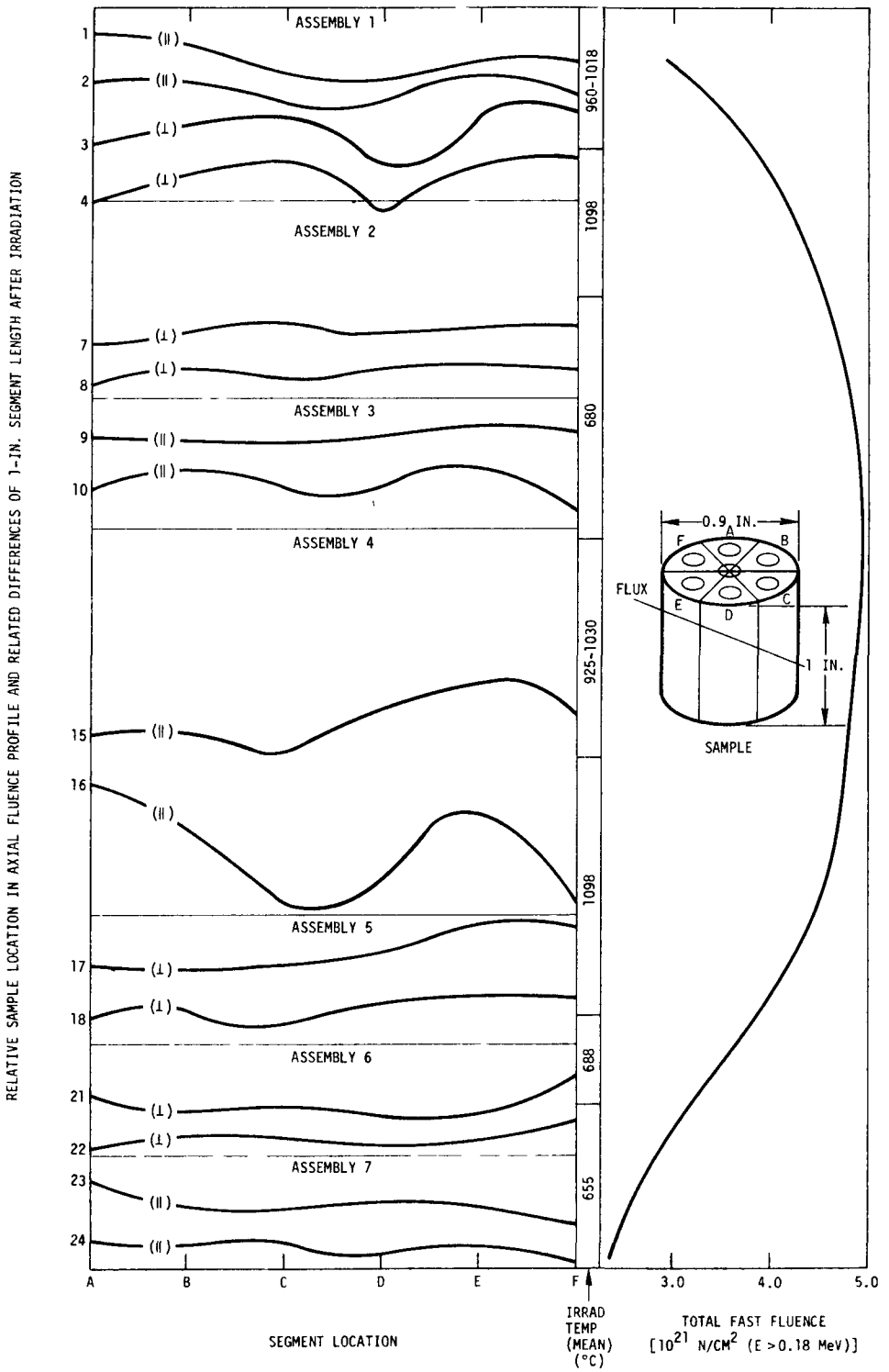

Fig. 7. Dimensional change differences resulting from flux gradients across section of segmented cylindrical assemblies (capsule G13)

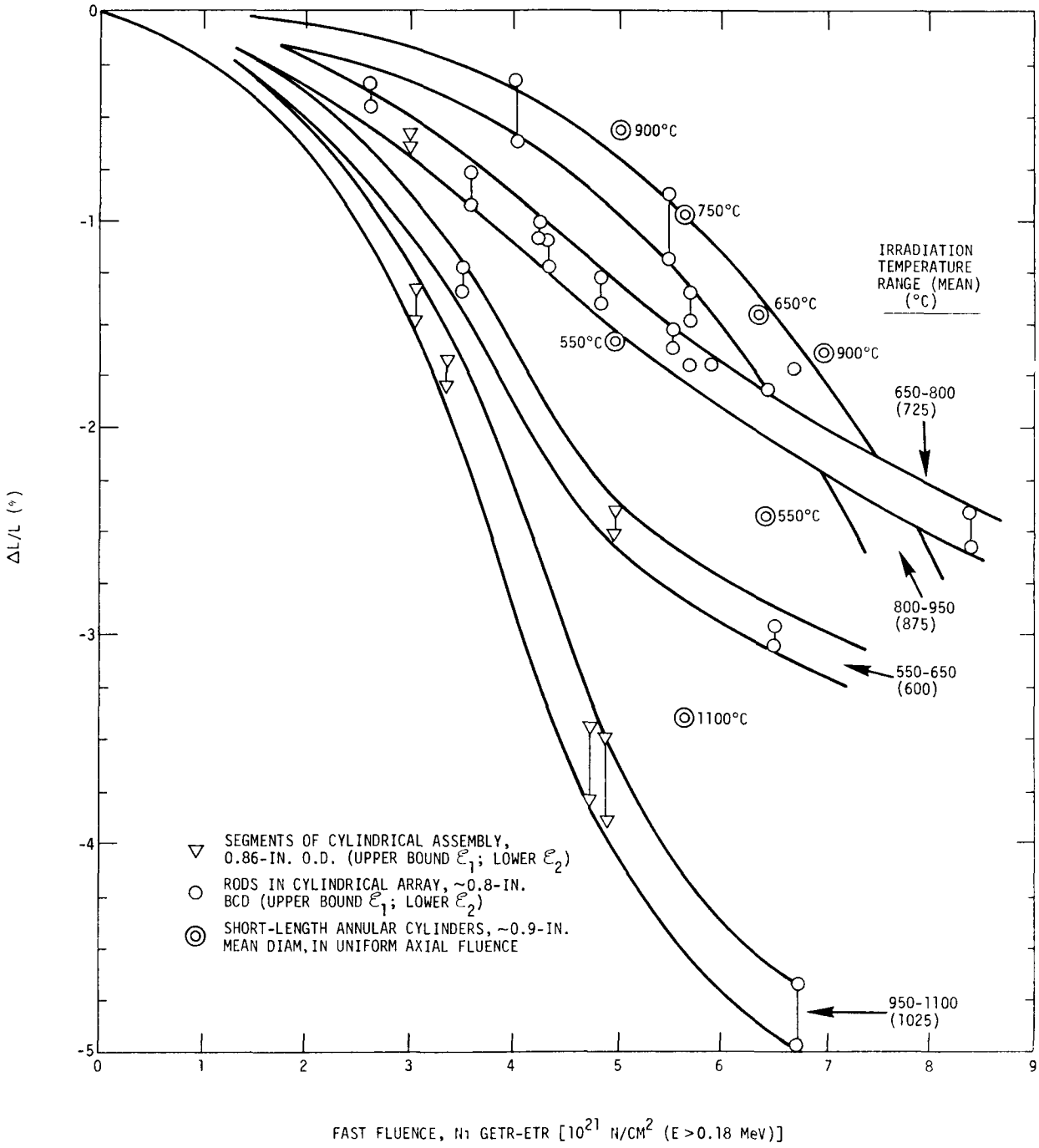

Fig. 8. Dimensional changes and dimensional change differences in cylindrical arrays of H-327 graphite (parallel orientation) due to 1-in. spatial fast flux gradient across the section

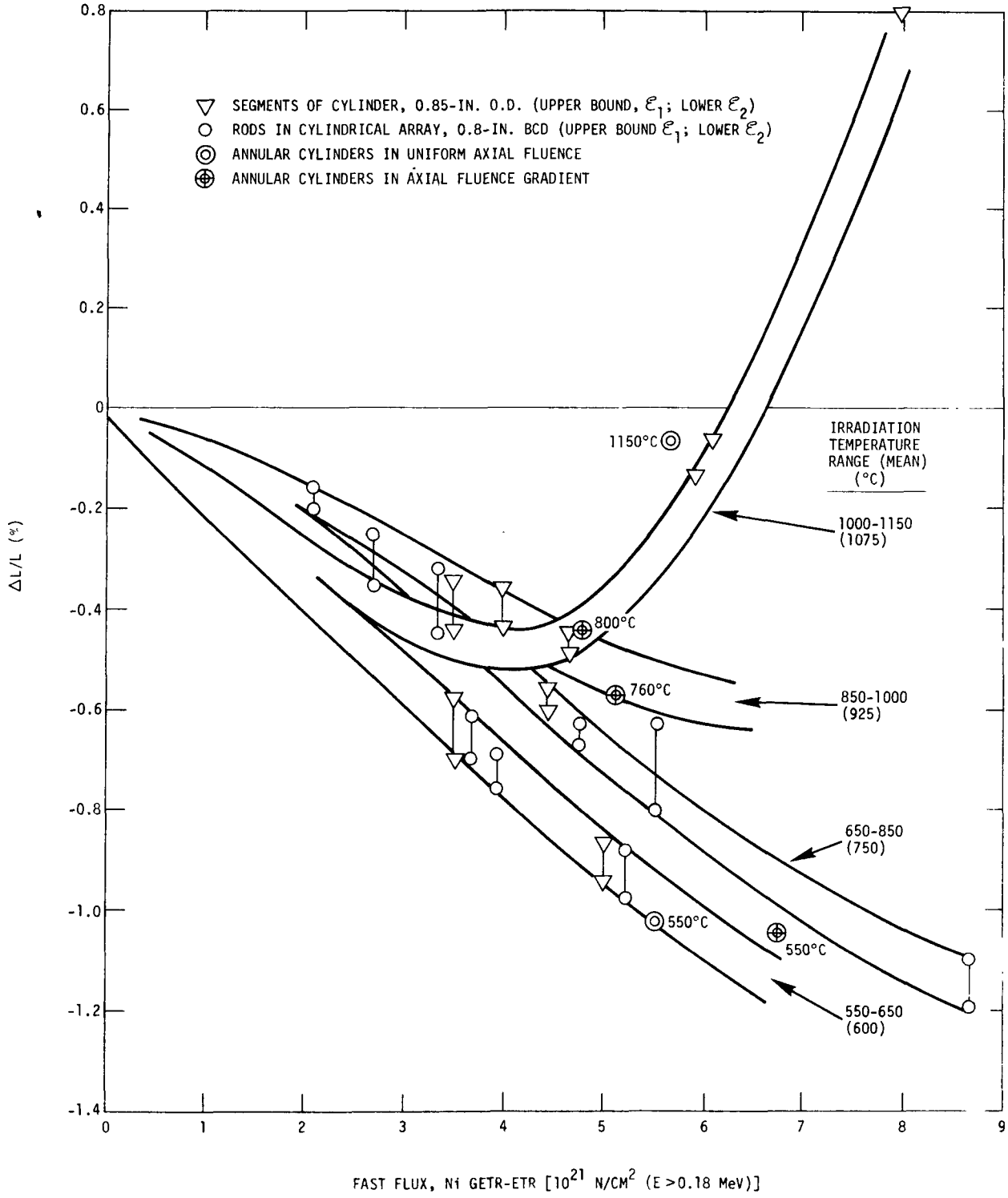

Fig. 9. Dimensional changes and dimensional change differences in cylindrical arrays of H-327 graphite (perpendicular direction) due to flux gradients

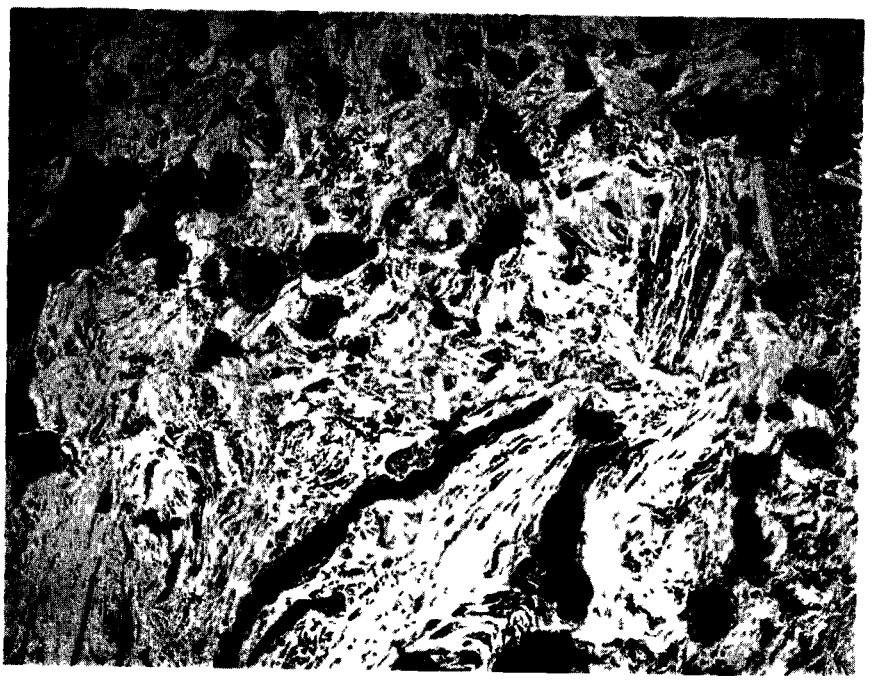

M31727-1 (a) 75x

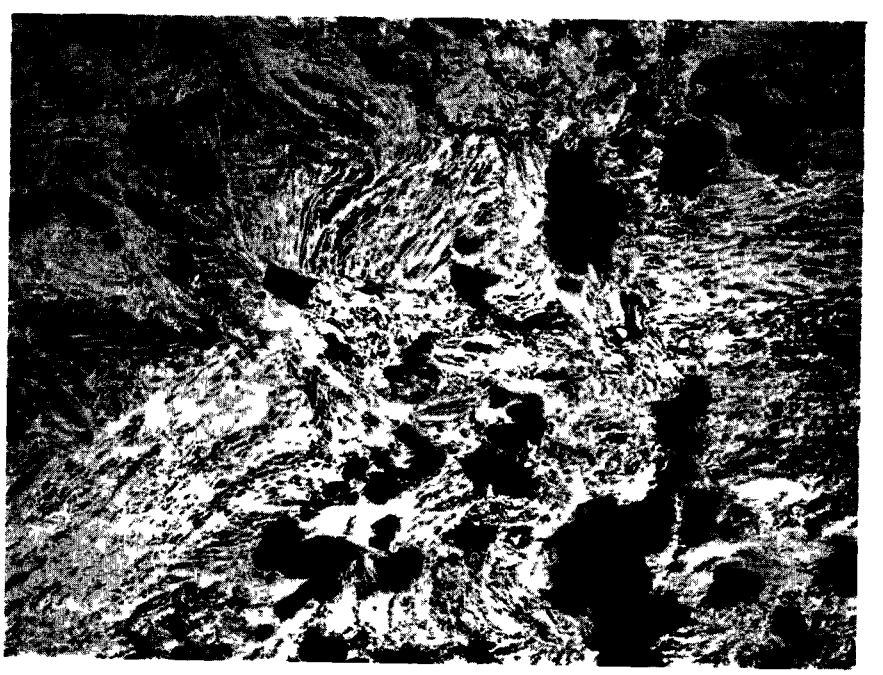

M31728-1 (b) 75x

Fig. 10. Structure of unirradiated H-327 graphite (FSV production grade): (a) parallel orientation; (b) perpendicular direction

M34252-2 (a) 75x

M34253-2 (b) 75x

Fig. 11. Structure of irradiated H-327 graphite rod, 0.105-in. diameter: (a) parallel orientation, 0.73% contraction, fluence = 3.7×10^{21} n/cm^2 (E > 0.18 MeV), temperature = 800°C; (b) perpendicular direction, 0.42% contraction, fluence = 3.7×10^{21} n/cm^2 (E > 0.18 MeV), temperature = 800°C

M34250-3 (a) 75x

M34251-1 (b) 75x

Fig. 12. Structure of irradiated H-327 graphite rod, 0.105-in. diameter: (a) parallel orientation, 1.80% contraction, fluence = 6.7×10^{21} n/cm^2 (E > 0.18 MeV), temperature = ∿650°C; (b) perpendicular direction, 0.95% contraction, fluence = 6.85×10^{21} n/cm^2 (E > 0.18 MeV), temperature = ∿650°C

5. DISCUSSION

An important feature in HTGR design and operation is the condition that may produce an unacceptable amount of expansion across the radius of the core. At the peak FSV graphite service temperatures of 1000° to 1150°C, H-327 graphite samples undergo approximately 0.5% maximum contraction in the direction across the core at 4.0×10^{21} n/cm^2 and then expand to produce a net increase in their original length at an estimated fluence of 6.5×10^{21} n/cm^2 (E > 0.18 MeV). The expansion rate from the turnaround point increases with increasing fluence and is doubled from values of

$$\frac{d(\Delta \ell/\ell)}{d(\phi t)} = 0.48$$

at the net expansion dose of 6.5×10^{21} n/cm^2 to approximately 1.0 at expected peak fluences of 8×10^{21} n/cm^2. It is thought that a relationship exists between the relatively small maximum contraction levels for H-327 material and the rate of increase in expansion for a given dose. The irradiation temperatures covered a range of 150°C in the graphite in the achievement of peak fluences, whereas FSV service temperatures are expected to oscillate less than 100°C. Assuming some inaccuracy of ±10% in dosimetry, crossover is not expected to occur before 6.3×10^{21} n/cm^2 (E > 0.18 MeV) at HTGR peak service temperatures. An equivalent ETR-GETR fluence value of 6.3×10^{21} n/cm^2 at energies greater than 0.18 MeV is considered a realistic dose level in the FSV core beyond which crossover (net expansion) in the fuel blocks at peak temperatures is likely to occur.

The dimensional change effects resulting from a finite change in the mean irradiation temperature as opposed to a swing in temperatures about a mean appear to be dependent upon the fluence and dimensional change rate and degree of dimensional change. Up to a fluence of 4×10^{21} n/cm^2

$$\frac{d(\Delta\ell/\ell)}{d(\phi t)}\ 1025°C \equiv \frac{d(\Delta\ell/\ell)}{d(\phi t)}\ 600°C \quad ,$$

and up to 7×10^{21} n/cm^2

$$\frac{d(\Delta\ell/\ell)}{d(\phi t)}\ 875°C \equiv \frac{d(\Delta\ell/\ell)}{d(\phi t)}\ 725°C \quad .$$

Thus, changes in irradiation temperature between the above paired values produce similar dimensional change trends. However, where the irradiation temperature changes (e.g., from 1025°C mean to 725°C), the subsequent rate of change is that for the lower temperature. There is a slightly lower contraction rate compared with material that has been constantly at this temperature which is thought to be influenced by the initial degree of change at the higher temperature. Turnaround in a sample of H-327 irradiated initially at peak FSV temperature and then at some lower value will occur at an intermediate fluence value. Crossover will, it is thought, be affected similarly, but since both fluences will be the lower bound case, they have no significance with regard to the intended life of H-327 graphite in the present HTGR design.

A significant aspect of the dimensional change data is that in all instances the irradiation contraction of the cylinders was less than that of the rods in cylindrical arrays or the segments assembled as cylinders. Any disparities due to temperature would have resulted in larger and smaller dimensional changes. A possible explanation is the creep effect due to differential contraction stresses. Whatever the disposition of the graphite and adjacent line source of neutrons, the damage power ϕ_D is a function of $(1/r)\Psi(r)$ in an infinite uniform graphite mass at a distance r from the source, $\Psi(r)$ being the damage function (Ref. 1). Any physical property change is an effect of the damage power ϕ_D, duration of irradiation t_o, and temperature θ_{irr} (Ref. 2). The irradiation times t_o of the samples in the arrays of rods and segmented assemblies are similar, and θ_{irr} is symmetrical about the center line of the assembly owing to the controlled cooling orifice around the samples. Thus, the physical property changes in the cylindrical assemblies of graphite specimens would be expected to change across the section, and it is reasonable to assume that the measured dimensional change differences are

due to this effect. The plots of dimensional changes in the H-327 rod and segment samples with respect to a measured fast neutron fluence, as shown in Figs. 8 and 9, are interpreted as ordinate increments for a given adjacent line fluence. The fluence range across the assembly is of the order of 10%, and the dimensional change differences reflect the uniaxial stress σ in the solid cylinders for a given value of Young's modulus E_{irr}, which changes with irradiation dose and temperature. It is therefore postulated that the size effect across the section of the cylinders produces an axial stress gradient due to a reduction in the damage power, and since the material is stronger in compression there is greater restraint of irradiation contraction than of expansion. The reverse situation occurs from the onset of turnaround, and the evidence of one test showing an approaching crossover at 6×10^{21} n/cm^2 ($E > 0.18$ MeV) fluence in a 1-in. thickness of graphite is considered the extreme case in regard to maximum FSV graphite thickness between neutron sources.

A method of conducting a restrained dimensional change experiment has been described by Losty and Orchard (Ref. 3) whereby a stress is obtained in a graphite body by making use of the differential shrinkages of two pieces of graphite. A creep constant K_a is derived which is the difference in restrained and unrestrained dimensional changes less the mechanical strain per damage fluence and average induced stress value. In comparing the dimensional changes of the cylinders and rods, any inherent restraint in the latter is taken into account by considering dimensional change differences E_r for the given damage gradient. The strain effects $\Delta\varepsilon$ are derived from the difference in dimensional change differences of the rods $(\varepsilon_2 - \varepsilon_1)$ in cylindrical arrays over the fluence range producing an average stress $\Delta\varepsilon(E_{rr}/2) = \sigma_{avg}$ due to a damage gradient effect γ for the adopted standard irradiation conditions of the capsules in the ETR and GETR.

The creep constant, or stress relaxation factor, is

$$K_{as} = \frac{E_r - (\Delta\varepsilon)}{\sigma_{avg}\gamma} \quad .$$

A first approximation of values for H-327 graphite can be derived over the approximately linear portion of the dimensional change curves (Fig. 8), where there are only single crucible data points, and between any consecutive crucible data points, where the curve is approximately linear. The limited data give a plot of creep constant versus irradiation temperature for H-327 complementary to plots of Kennedy's AGOT data (Ref. 4) and of results derived by Petten (Ref. 5)(Fig. 13).

It is also worthy of note that H-327 graphite showed no apparent loss in integrity as evidenced by the superficial appearance of the irradiated samples at doses beyond 8×10^{21} n/cm^2 (E > 0.18 MeV). Furthermore, the microstructure appears to be relatively unchanged at the peak dimensional change conditions to be expected in the FSV fuel elements.

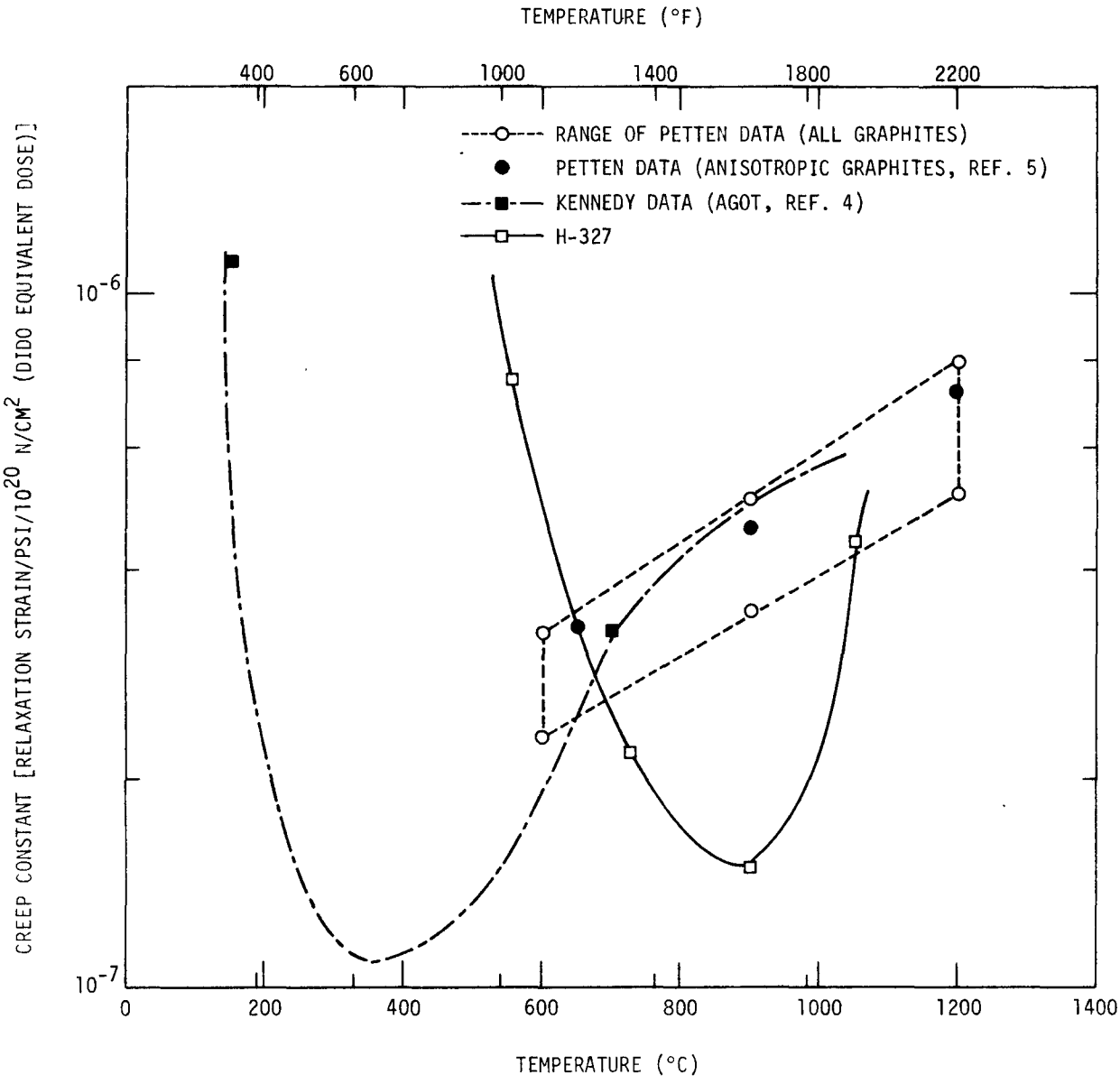

Fig. 13. Irradiation stress relaxation effects for a number of reactor graphites expressed as a creep constant spanning FSV temperatures

6. CONCLUSIONS

Expansion in the radial direction of a FSV first core fuel block will not occur before a minimum fast fluence of 6.3×10^{21} n/cm^2 (E > 0.18 MeV) at the higher operating temperatures of the H-327 graphite. From the onset of expansion the rate is steep so that at 8×10^{21} n/cm^2 (E > 0.18 MeV), a net radial length increase (perpendicular to the graphite extrusion direction) of 0.8% (8 mils per inch) is probable at 1100°C. The maximum shrinkage in an H-327 fuel block is estimated to be 1.2% (12 mils per inch) at temperatures of 550° to 650°C and 1.1% (11 mils per inch) at 650° to 850°C at the peak FSV fluence of 8×10^{21} n/cm^2 (E > 0.18 MeV).

The maximum contraction in the length of a FSV fuel block will be 5% to 6% (50 mils per inch) at the peak operating conditions of 950° to 1100°C at a fluence of 7 to 8×10^{21} n/cm^2. The H-327 fuel block material operating below these temperatures will undergo approximately half this amount of contraction.

It is believed that the fluence or damage gradient across a graphite section influences the subsequent dimensional changes. The range of dimensional changes induced in 0.1- to 1.0-in.-diameter production grade H-327 graphite samples currently irradiated in the ETR or GETR covers the range of graphite web thicknesses between any adjacent fuel positions in FSV fuel elements.

The effects of changes in mean irradiation temperatures are related to the similarities in dimensional change rates of the respective temperatures, at least up to turnaround conditions in the parallel direction. Where large temperature changes are made, as would exist in any axial fuel or spectral shuffling, the dimensional change rate complements the new temperature effects.

Damage gradients in the radial direction of a longitudinal irradiation sample affect the subsequent length changes in the specimen by a condition of axial stress which induces a stress relaxation or creep effect. The creep constant derived as a first approximation from dimensional change differences in 1-in.-diameter cylinders and small-diameter rods pitched on a similar diameter is comparable to the general range of values derived for anisotropic materials. The curve of creep coefficient versus irradiation temperature is similar in form but undergoes a shift of a factor of two increases in the temperature when compared with the curve for AGOT, a similar type of graphite.

ACKNOWLEDGMENTS

The author gratefully acknowledges the work of the various members of the GGA Irradiation and Hot Cell Groups, and also the work by Jim Audas and Dwight Davis of the HTGR Core Materials Branch, who performed the preirradiation and postirradiation dimensional measurements.

REFERENCES

1. Bell, J. C., et al., "Stored Energy in the Graphite of Power-Producing Reactors," Phil. Trans. Roy. Soc. (London) A254, 361 (1962).
2. Simmons, J. H. W., Radiation Damage in Graphite, Pergamon Press, Oxford, 1965, p. 102.
3. Losty, H. H. W., and J. S. Orchard, "The Strength of Graphite," in Proceedings of the Fifth Conference on Carbon, Vol. 1, Pergamon Press, New York, 1962, p. 519.
4. Savolainen, A. W. (ed.), "Gas-Cooled Reactor Program. Semiannual Progress Report for Period Ending September 30, 1966," USAEC Report ORNL-4036, Oak Ridge National Laboratory, 1967.
5. Blackstone, R., L. W. Graham, and M. R. Everett, "High Temperature Radiation Induced Creep in Graphite," Dragon Project Report D.P.-Report-665, 1969.